Automated Highway Lane Changes of Long Vehicle Combinations: A Specific Comparison Between Driver Model Based Control and Non-linear Model Predictive Control

Peter Nilsson[*], Leo Laine[*], Niels van Duijkeren[†] and Bengt Jacobson[‡]

[*]Department of Chassis Strategies & Vehicle Analysis
Volvo Group Truck Technology, BF72991, AB4S, SE-405 08, Göteborg, Sweden
Email: peter.q.nilsson@volvo.com, leo.laine@volvo.com

[†]Department of Mechanical Engineering, Division PMA
KU Leuven, 3001 Heverlee, Belgium
Email: niels.vanduijkeren@kuleuven.be

[‡]Vehicle Dynamics group, Division of Vehicle Engineering & Autonomous Systems, Department of Applied Mechanics
Chalmers University of Technology, SE-412 96, Göteborg, Sweden
Email: bengt.jacobson@chalmers.se

Abstract—This paper compares the vehicle dynamics performances of two approaches for automated lane change manoeuvres of a long vehicle combination in simulated highway driving. One of the two approaches is a non-linear model predictive controller (NMPC), and the other is based on driver model control (DMC) theory. Both approaches utilize traffic situation predictions that include motion variable constraints and actuation requests for steering, propulsion and braking. The two automated driving approaches are compared in a simulation environment including a high-fidelity vehicle plant model and models of surrounding vehicles. Simulations show that both approaches can generate feasible lane change manoeuvres at the constant speeds of 44 and 78 km/h. In addition, lane changes were successfully conducted in combination with retardation due to leading vehicle braking from 80 to 50 km/h with a varying retardation range of 0.1-0.7 g. In general, the non-linear model predictive control shows a shorter lane change duration and lower values of the used absolute magnitude of the longitudinal and lateral accelerations. However, the specific objective function used in the NMPC leads to an unnecessary variation of longitudinal vehicle speed compared to the driver model control approach.

I. INTRODUCTION

Long vehicle combinations (LVCs), such as illustrated in Figure 1, refer to modular road vehicles that are longer and heavier than the currently permitted dimensions in Europe. The main motivating factors for LVC utilization are increased vehicle productivity and reduced environmental impact. However, by using LVCs the lateral vehicle dynamics in high speed manoeuvres such as lane changes, can be further amplified in comparison to current vehicle combinations and therefore possibly impair road traffic safety. Typical performance characterics for LVCs are rearward amplification of the lateral acceleration between the first and last vehicle units and lateral off-tracking between the first and last axles in the vehicle combination [1].

A promising approach for improving the road traffic safety of LVCs is the utilization of advanced driver assistance systems including fully or partially automated steering, propulsion and braking. However, automation with a human occupant in the cabin gives rise to the fact that human comfort will add constraints on the automated system. One way of quantifying the needed level of comfort is to introduce the concept of *satisficing* behaviour [2]. Satisficing is here defined as the 'comfort zone' where the driver is content with good-enough behaviour. It should be noted that comfort here refers to attributes such as being relaxed, safe and the feeling of being in control.

There are several methods for generating collision-free trajectories presumably needed for automated driving. Some of these methods don't include a model of the subject vehicle, e.g. the graph-based method A* [3] which has been used within robotics. However, the LVC application is a non-holonomic system [4], in simple terms, a system whose states depend on the path taken in order to achieve it. Control methods that don't explicitly predict future trajectories are not considered suitable for LVCs. Some manoeuvres need to be properly prepared to ensure feasibility. Consider, for example, braking before a corner or taking wider corners to prevent trailers from leaving the road. A distinction is often made between two kinds of predictive techniques, the first employs online optimization [5] whereas the other implements (randomized) sampling based approaches such as Rapidly-exploring Random Trees [6]. For both approaches it is not necessarily obvious how to choose the objective and constraints for satisficing driving behaviour. In this work, two specific approaches for the automated driving of LVCs have been compared with regards to vehicle dynamics performance and its possible influence on a satificing driving experience. One of the two approaches is a non-linear model predictive controller (NMPC), and the other is based on driver model control (DMC) theory. Both approaches utilize a subject vehicle prediction model to generate traffic predictions that include actuation requests for steering and propulsion and motion variable constraints. The specific settings of the controllers were used in a moving base driving simulator study [7]. The objective in developing the approaches, both regarding formulation and parameter settings, was to meet a satisficing behaviour for the human occupant. In the DMC approach, the used driver model for longitudinal and lateral control was inspired by human cognition and optic flow theory. This basis is envisioned to provide a control performance which has an inherent satisficing behaviour. To the best knowledge of the authors, a combined longitudinal and lateral driver model

Fig. 1: An example of a LVC. The illustrated vehicle is referred to as an A-double combination.

Fig. 2: Function reference architecture: solid boxes are explained, dashed boxes are only for orientation.

based on visual information in combination with traffic predictions, has never before been used for realizing and evaluating lane changes of LVCs, as is shown in this paper. The NMPC solution techniques, which often are computationally intensive, are becoming a viable option for real-time implementation [8]. When studying human driving behaviour for LVCs [9] it was found that drivers minimise the total acceleration changes, which is here included as a part of the cost function in the NMPC.

II. MODELLING

In this section the mathematical models used for predictions, control design and emulation of the subject and surrounding vehicles are presented.

A. Subject vehicle prediction model

The LVC motion in the controller predictions is described using a one-track model with a linear tyre constitution and assumes small steering, articulation and side-slip angles. The model formulation and parameters are based on [10]. The differential equations which constitute 16 states and 2 inputs are given in the Appendix. In order to calculate the position of the LVC and its units with respect to the road, a parametrization of the road curvature and heading are included in the model equations.

B. Subject vehicle plant model

A high fidelity two-track model library developed at Volvo Group Truck Technology (VGTT), is used to emulate the LVC plant model dynamics. The library includes detailed submodels of the vehicle chassis, cab suspension, steering system, powertrain, and brakes. The Magic Formula tire model [11] with combined slip, dynamic relaxation, and rolling resistance, is used to describe the constitutive relations for all tires in the vehicle combination.

C. Surrounding vehicle prediction and plant model

The motion of the surrounding vehicles are described using point-mass models including predetermined acceleration profiles. The resulting differential equations are given in the Appendix. Besides the defined states the vehicles also include information of their spatial dimensions and the current lane identity. When the model is used in the traffic situation predictions, a constant velocity is assumed during the entire prediction horizon.
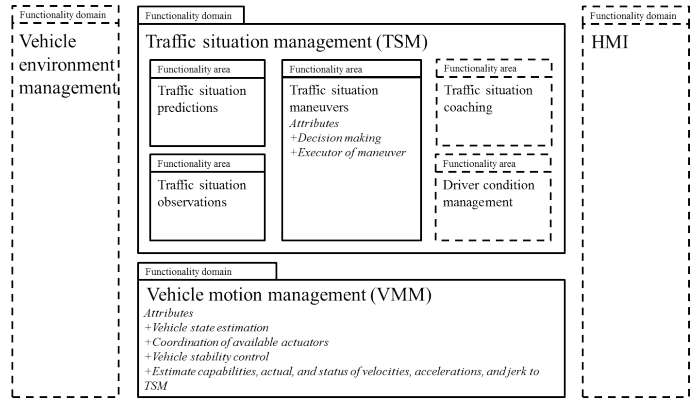
III. ARCHITECTURE FOR VEHICLE MOTION FUNCTIONALITY

The vehicle's motion functionality was partitioned and developed with regards to a function reference architecture which is used within VGTT, see Figure 2. The partitioning was done into a hierarchical structure to separate motion functionality in long term, mid term, and short term planning, execution, and tracking. This was because it is foreseen that different spatial and time horizon predictions and planning will be conducted which requires modelling with different granularity of the subject vehicle and the surrounding environment for efficient computations in the intended time and spatial horizon [12]. In addition, the reference architecture also addresses that internal quality attributes such as adaptability, changeability, and stability are achieved [13]. The external quality attributes of the architecture such as interoperability and functional behaviour need to be evaluated by simulations and physical testing [13]. The functionality domain (FD) vehicle motion management (VMM) has a time horizon of up to 1 s and has reactive and coordinative character with vehicle stability as a core functionality. The FD traffic situation management (TSM) has a time horizon of up to 10 s and the prediction has a tactical character. The FDs of strategical character, with a time horizon larger than 10 s, are omitted. The VMM FD encapsulates the knowledge of specific available actuation topology within the vehicle combination. The main attributes are vehicle state estimation and transforming acceleration or speed requests into available actuation requests. In the current approaches, control allocation has been used for coordinating propulsion, braking, and steering [14]. The control allocation weighting for, e.g. braking in-between axles, has been adapted to commercial heavy vehicles [15]. The control allocation formulation has also been adapted for large articulation angles between the vehicle units and wheel steer angles by deriving the actuation control efficiency matrix $B(\theta_i, \delta_j)$ by using Lagrange formulation [16]. Within the TSM FD there are three main functionality areas: traffic situation observation, traffic situation predictions, and traffic situation manoeuvres. Further details about the reference architecture are found in [17].

$[\kappa_r], [\theta_r], [s_r], [v_{r,max}]$
$[\Delta s_{o,n}], [\dot{s}_{o,n}], [\ddot{s}_{o,n}], [l_{o,n}]$
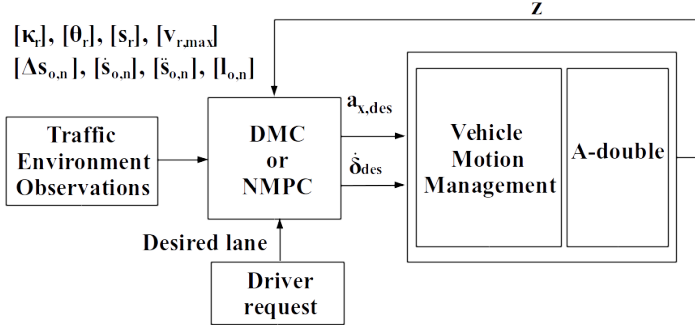
Fig. 3: Control design of automated driving. The inputs for the DMC and NMPC are: state measurements z and traffic environment observations including; road curvature $[\kappa_r]$, road heading angle $[\theta_r]$, road distance $[s_r]$ and max road velocity $[v_{r,max}]$. Also, the relative distance $[\Delta s_{o,n}]$, velocity $[\dot{s}_{o,n}]$, acceleration $[\ddot{s}_{o,n}]$ and lane $[l_{o,n}]$ of surrounding vehicles. The outputs are the desired longitudinal acceleration $a_{x,des}$ and road wheel steering angle rate $\dot{\delta}_{des}$.

IV. CLOSED-LOOP CONTROL DESIGN

In this section the control design for automated driving is presented. The closed-loop control schedules for the DMC and the NMPC approach are illustrated in Figure 3.

A. Driver model control

A combined longitudinal and lateral driver model is used for the LVC motion guidance and follows the approach presented in [17]. The model parameters are illustrated in Figure 4.
In order to manage the automated driving task, three traffic situation predictions, corresponding to the LVC lane and the adjacent left and right lanes, are performed. The predictions are carried out as closed-loop simulations including the driver model and prediction models of the LVC and the surrounding vehicles. The simulations of the predictions are done using the forward Euler method with step size and prediction times of 0.05 s and 3.75 s, respectively. The closed-loop control frequency is synchronized with the DMC control intervals and is updated at a control rate of 40 Hz. For each step in the simulations, the predictions are evaluated regarding constraints related to vehicle dynamics, lane boundaries and distance to surrounding vehicles according to

$$\underline{v}_x \leq v_{x,1} \leq \overline{v}_x \tag{1}$$

$$\underline{a}_y \leq a_{y,i} \leq \overline{a}_y \tag{2}$$

$$s_{o,j,leading} \geq s_1 \tag{3}$$

$$s_{o,j,trailing} \leq s_{11} \tag{4}$$

$$\underline{e}_{j,k} \leq e_i \leq \overline{e}_{j,k} \tag{5}$$

$i = 1, 11$ are the numbers of the axles in the vehicle combination
$j = 0, 1, 2$ are the number of the predictions
$k = 1, ..., 11$ are number of the current driving state

where $\underline{v}_x$ and $\overline{v}_x$ are the vehicle speed limits and $v_{x,1}$ is the speed of the first LVC axle. Furthermore, $\underline{a}_y$ and $\overline{a}_y$ are the lateral acceleration limits, $a_{y,1}$ and $a_{y,11}$ are the lateral accelerations of the first and last LVC axles. The distances $\underline{e}_{j,k}$ and $\overline{e}_{j,k}$ are the limits of the perpendicular distances from the lane center line. $s_{o,j,leading}$ and $s_{o,j,trailing}$ are the distances to the leading and trailing vehicles, s_1, s_{11}, e_1 and e_{11} are the distances

and perpendicular distances of the first and last LVC axles projected on the lane geometry. The upper and lower values of the constraints related to the lane boundaries are dependent on the current driving state. If any constraint is violated, the prediction is identified as infeasible, which is used in decision making, e.g. decision to change lane or emergency brake. How the predictions are combined with decision making in the TSM is further explained in [17]. However, the simulation scenarios in this paper are selected for having a minimal affect through decision making in the DMC and NMPC approach.

1) Longitudinal control: The longitudinal control part of the driver model, based on [18], is formulated as an iteratively updated feed-forward controller (6), using a reference acceleration $a_{x,ref}$ to maintain constant $\dot{\tau}_m$. The margin values described and calculated in (7)-(8) are used for control action switching.

$$a_{x,ref} = (1 + \dot{\tau}_m) \cdot \frac{\Delta v_x^2}{(\Delta X_f - v_o \cdot t_h)} \tag{6}$$

$$\underline{a}_x \leq a_{x,ref} \leq \overline{a}_x$$

In Equation (6), Δv_x is the speed difference between the LVC front axle and the lead vehicle, ΔX_f is the far point distance, and t_h is the desired final temporal headway. The constant parameter $\dot{\tau}_m$ is an approximation of the time derivative of time-to-collision. The magnitude of $a_{x,ref}$ is constrained by the lower $\underline{a}_x$ and upper limits $\overline{a}_x$. In addition, the retardation and acceleration are ramped up to their requested values using a limit on the jerk magnitude during initial braking and propulsion.
The initiation of braking and propulsion utilizes margin values of the optical expansion rate $\dot{\theta}_{p,m}$ and the temporal headway to the leading vehicle $t_{hl,m}$.

$$\dot{\theta}_{p,m} \leq \dot{\theta}_p \leq -\dot{\theta}_{p,m} \tag{7}$$

$$t_{hl,m} + \varepsilon_t \leq t_h \leq t_{hl,m}$$

where ε_t is a small constant parameter. The optical expansion rate $\dot{\theta}_p$ and the temporal headway t_h are calculated as

$$\dot{\theta}_p = \frac{-4 \cdot w \cdot \Delta v_x}{w^2 + 4 \cdot \Delta X_f^2} \tag{8}$$

$$t_h = \frac{\Delta X_f}{v_{x,1}}$$

where w is the width of the leading vehicle and $v_{x,1}$ is the speed of the LVC front axle.

2) Lateral control: The lateral control part of the driver model is based on a two-point visual model [19] formulated as

$$\dot{\delta}_{des} = k_f \cdot \dot{\theta}_f + k_n \cdot \dot{\theta}_n + k_I \cdot \theta_n \tag{9}$$

where $\dot{\delta}_{des}$ is the time derivative of the desired steering wheel angle, θ_n is the perceived angle to a near point, and $\dot{\theta}_f$ and $\dot{\theta}_n$ are the angular velocities of the perceived angles to a far and near point, respectively, see Figure 4. The values of gain factors, k_f, k_n and k_I were parametrized using a genetic algorithm [20] and lane change measurement data for a constant vehicle speed of 80 km/h [21].

B. Non-linear model predictive control

The NMPC technique for longitudinal and lateral control used for the LVC's motion guidances is based on [8]. The original variable notation has been retained to facilitate backward
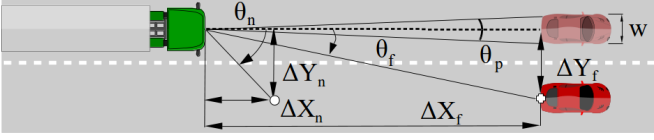
Fig. 4: Optical parameters used in the driver model: optical size $\theta_{\rm p}$, angle to a near-point $\theta_{\rm n}$, and a far-point $\theta_{\rm f}$. The distance w is the width of the lead vehicle and $\Delta X_{\rm n}$ and $\Delta X_{\rm f}$ are the distances to the near and far-points, respectively.

referencing. A constrained optimal control problem (OCP) is formulated which describes the desired motion of the LVC over a finite future horizon. The OCP is transcribed into a non-linear program (NLP) using a multiple shooting prediction model integration technique. Real-time performance is achieved using the real-time iteration (RTI) scheme proposed in [22].

1) Optimal control problem formulation: For the automated driving task, three possibly conflicting objectives are identified. The first part is a lane center-line distance offset tracking objective, the second part promotes smooth and comfortable driving, and the third part penalizes driving close to surrounding vehicles. The components of the cost function attempt to result in satisficing solutions for the human occupant. The infinite dimensional optimal control problem and its constraints are formulated as

$$\min_{\xi(\cdot),u(\cdot)} \int_{s=0}^{s_f} \left(K_{d_1} ({}^{af}_{\Phi}d^{\Phi} - {}^{af}_{\Phi}d^{\Phi}_{\rm ref})^2 + K_{d_4} ({}^{dr}_{\Phi}d^{\Phi} - {}^{dr}_{\Phi}d^{\Phi}_{\rm ref})^2 \right.$$
$$+ K_{v_x} ({}^{ac}_{Z}v^{Ac}_x - {}^{ac}_{Z}v^{Ac}_{x,\rm ref})^2 + K_{j_x} ({}^{ac}_{Z}j^{Ac}_{x,\rm des})^2$$
$$+ K_{j_y} ({}^{ac}_{Z}j^{Ac}_y)^2 + K_{a_x} ({}^{ac}_{Z}a^{Ac}_{x,\rm des})^2$$
$$\left. + K_{\dot\delta}\dot\delta^2 + \sum_{k=1}^{3} K_{\Delta s_{o,k}} \left(f_{\rm dk}(\Delta s_{o,k}, {}^{af}_{Z}v^{Af}_x) \right)^2 \right) d\sigma \tag{10}$$

$$\frac{d\xi}{ds} \qquad = f(s,\xi,u) \tag{11}$$

$$\underline{a}_y \qquad \le {}^{af}_{Z}a^{Af}_y(s) \qquad \le \overline{a}_y \tag{12}$$
$$\underline{a}_y \qquad \le {}^{dr}_{Z}a^{Dr}_y(s) \qquad \le \overline{a}_y \tag{13}$$
$$\underline{d} \qquad \le {}^{af}_{\Phi}d^{\Phi}(s) \qquad \le \overline{d} \tag{14}$$
$$\underline{d} \qquad \le {}^{dr}_{\Phi}d^{\Phi}(s) \qquad \le \overline{d} \tag{15}$$
$$\underline{a}_{x,\rm des} \qquad \le {}^{ac}_{Z}a^{Ac}_{x,\rm des}(s) \qquad \le \overline{a}_{x,\rm des} \tag{16}$$
$$\underline{\delta} \qquad \le \delta(s) \qquad \le \overline{\delta} \tag{17}$$
$$\underline{\dot\delta} \qquad \le \dot\delta(s) \qquad \le \overline{\dot\delta} \tag{18}$$
$$\underline{\Delta s}_{o,k} \qquad \le \Delta s_{o,k} \qquad k = 1,\ldots,3 \tag{19}$$
$$\forall s \in [0, s_f]$$

where ${}^{af}_{\Phi}d^{\Phi}$ and ${}^{dr}_{\Phi}d^{\Phi}$ are the lateral distances offset along the road geometry of the first and last axle of the LVC, respectively. The variables ${}^{ac}_{Z}v^{Ac}_x$, ${}^{ac}_{Z}a^{Ac}_{x,\rm des}$ and ${}^{ac}_{Z}j^{Ac}_{x,\rm des}$ are the longitudinal velocity, desired acceleration and jerk expressed relative to a local coordinate frame positioned in the center of gravity of the first LVC unit. The variable ${}^{ac}_{Z}j^{Ac}_y$ is the lateral jerk at the center of gravity of the first LVC unit and $\dot\delta$ is the steering angle rate. The term $f_{\rm dk}(\Delta s_{o,k}, {}^{af}_{Z}v^{Af}_x)$ is related to the distance keeping. K_{d_1}, K_{d_4}, K_{v_x}, K_{j_x}, K_{j_y}, K_{a_x}, $K_{\dot\delta}$ and $K_{\Delta s_{o,k}}$ are gain factors. The equations of motion (11) depend on the position of the front axle of the tractor along the road geometry

${}^{af}_{\Phi}s^{\Phi}$, the state ξ, and the control input u. Constraints (12) and (13) limit the lateral accelerations of two positions of the LVC to prevent the LVC from rolling over. Constraints (14) and (15) enforce two positions of the LVC to stay inside the lane boundaries. Constraint (16) informs the trajectory generator of the physical maximum longitudinal acceleration of the LVC. The constraints (17) and (18) reflect the maximum road wheel angle and its time derivative, respectively, reflecting physical actuation constraints. Finally, (19) prohibits a trajectory that collides with that of one of the surrounding vehicles.

The logic governing which surrounding vehicles to consider in the OCP is largely implemented in a preprocessing stage to the OCP solver. Constraint 19 is introduced for each vehicle and longitudinal distance keeping is promoted by the quadratic penalty

$$\sum_{k=1}^{3} K_{\Delta s_{o,k}} \left(f_{\rm dk}(\Delta s_{o,k}, {}^{ac}_{Z}v^{Ac}_x) \right)^2 \tag{20}$$

where the function $f_{\rm dk}$ approximates the logic sensitivity of the optimal solution with respect to the temporal distance to other vehicles with a sigmoid function. Further details on the optimal control problem formulation are found in [8].

2) Solution techniques: The OCP problem introduced in Section IV-B1 is transcribed into a NLP using the ACADO toolkit [23]. The spatial prediction horizon in ${}^{af}_{\Phi}s^{\Phi}$ is discretized using 50 intervals with a step size Δs of 2 m. The dynamic constraints are imposed with a multiple-shooting integration scheme using a fourth order explicit Runge-Kutta update rule taking 5 intermediate integration steps in each discretization interval of the OCP. The used horizon length and the control frequency are 100 m and 2 m^{-1}, respectively. The closed-loop control frequency is synchronized with the NMPC control intervals of the translated OCP and is triggered every 2 m travelled along the lane center-line. When driving with the speed 72 km/h this corresponds to a control rate of 10 Hz.

V. SIMULATION RESULTS

The simulation results from two lane change scenarios are presented in this section. Both scenarios are on a straight three lane one-way road with two surrounding vehicles in each lane. A straight road was selected for clarity when presenting the results. The specific scenario and control parameters used in the simulations are given in Table I.

In the first scenario, lane changes to the right are carried out at the constant LVC velocities of 44 and 78 km/h. In the case when the LVC velocity is 78 km/h the headways to the leading and trailing vehicles are 2 s and 6 s, respectively. When the LVC velocity is 44 km/h the headways to the leading and trailing vehicles are 2 s and 9 s, respectively. The headway is kept constant until the scenario starts at the time 17 s. When the scenario is started, the velocities of the surrounding vehicles are kept constant. The initial conditions of the scenario are illustrated in Figure 5 (top).

In the second scenario, lane changes to the right are combined with braking. The initial LVC velocity is 80 km/h. The headways to the leading and trailing vehicles are 2 s and 7 s, respectively. The initial conditions regarding the leading vehicles are the same as in the first scenario. However, when the first axle of the LVC enters the target lane the leading
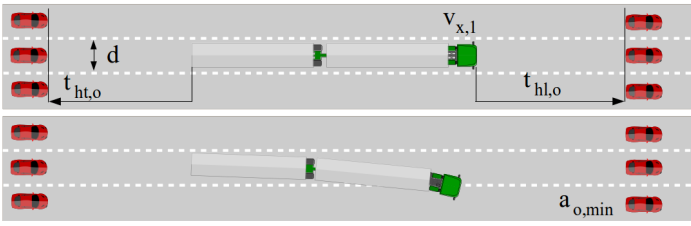
Fig. 5: The top panel illustrates the initial conditions for both lane change scenarios. The bottom panel shows the condition in scenario II for when the leading vehicles starts decelerate.

TABLE I: Parameters used in the scenarios and in the DMC and NMPC.

Scenario I parameters	Symbol	Value	Unit
LVC velocity	$v_{x,1}$	44., 78.	km/h
Temporal headway leading vehicles	$t_{hl,o}$	2., 2.	s
Temporal headway trailing vehicles	$t_{ht,o}$	9., 6.	s
Start of scenario	t_{in}	17.	s
Lane change requested	t_{lc}	20.	s
Lane width	d	4.	m
Scenario II parameters			
Initial LVC speed	$v_{x,1,init}$	80.	km/h
Final LVC speed	$v_{x,1,final}$	50.	km/h
Axle offset for start of lead retardation	$e_{1,start}$	-2.	m
Initial temporal headway leading vehicles	$t_{hl,o}$	2.	s
Initial temporal headway trailing vehicles	$t_{ht,o}$	7.	s
Lead vehicle retardation	$a_{o,min}$	0.1, 0.3, 0.5, 0.7	g
Lane width	d	4.	m
DMC parameters			
Maximum LVC acceleration	$\underline{a}_{x,des}, \overline{a}_{x,des}$	-5.9, 0.3	m/s^2
Lateral acceleration limit	$\underline{a}_y, \overline{a}_y$	-3., 3.	m/s^2
Tau rate	$\dot{\tau}_{s,m}$	-0.425	-
Optical expansion rate margin value	$\theta_{p,m}$	0.2	°/s
Gain perceived angle rate, far point	k_f	3.07	-
Gain perceived angle rate, near point	k_n	1.48	-
Gain perceived angle, near point	k_I	0.41	-
Near point distance	x_n	5.	m
NMPC parameters			
Cost function weight factors			
Lateral distance offset 1st axle	K_{d_1}	400.	-
Lateral distance offset 11th axle	K_{d_4}	200.	-
Lateral jerk	K_{j_y}	50.	-
Vehicle speed	K_{v_x}	2.	-
Longitudinal acceleration	K_{a_x}	11.4	-
Steering wheel angle rate	K_δ	20.	-
Longitudinal jerk	K_{j_x}	25.	-
Distance to surrounding vehicles	$K_{\Delta s_{o,k}}$	4167.	-
Constraint limits			
Maximum LVC acceleration	$\underline{a}_{x,des}, \overline{a}_{x,des}$	-2.5, 0.25	m/s^2
Lateral acceleration limit	$\underline{a}_y, \overline{a}_y$	-2.5, 2.5	m/s^2
Steering wheel angle limit	$\underline{\delta}, \overline{\delta}$	-103., 103	°
Steering wheel angle rate limit	$\underline{\dot{\delta}}, \overline{\dot{\delta}}$	-51.5, 51.5	°/s

vehicles starts braking, illustrated in Figure 5 (bottom). At this point, the LVC needs to combine steering and braking in order to fulfil the initiated lane change. The deceleration of the leading vehicles are varied in the range of 0.1-0.7 *g*.

The simulations are carried out in a Matlab/Simulink environment. The high-fidelity vehicle model, the road description and the motion of the surrounding vehicles are modelled in Simulink. The control systems, which are written in C/C++, are interfaced using a Matlab s-function.

A. Scenario I: Lane change at constant speed

In this section the performance of the DMC and the NMPC approaches are compared for lane changes at the constant velocities of 44 and 78 km/h. Important characteristics of the lane changes are shown in Figures 6-9. The top and bottom rows of each Figure illustrate the performance of the DMC and the NMPC, respectively.
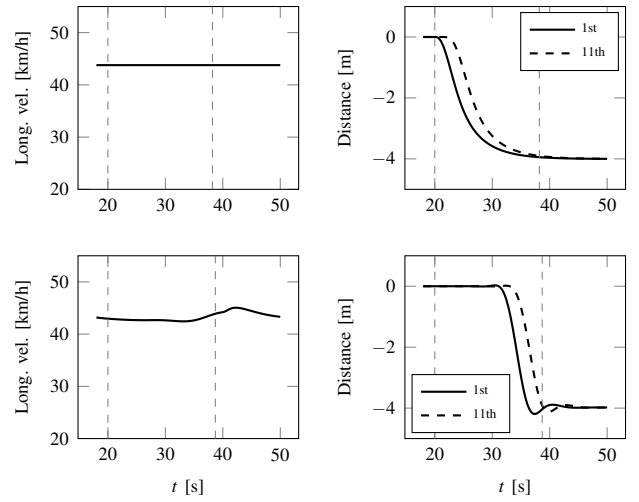
Fig. 6: Characteristics of a lane change at the constant velocity of 44 km/h: vehicle speed DMC (top left), lane center distance offset DMC (top right), vehicle speed NMPC (bottom left), and lane center distance offset NMPC (bottom right). The dashed vertical lines indicate lane change initiation and completion.

In both scenarios, a lane change to right is requested at time 20 s. The DMC approach initiates the lane changes immediately while the NMPC starts the lane changes at 28 and 21 s. The motivation behind this delay in the NMPC approach is to introduce the change of reference to the optimization in a controlled manner. The RTI scheme does not solve the entire NLP for each control interval and a sudden change of reference may temporarily lead to highly suboptimal control. Although convergence is typically very fast, it can compromise the satisficing experience for the driver. At the velocity of 44 km/h the lane change for both the DMC and the NMPC are completed at 38 s, occurring when the 1st and 11th axles of the LVC are within a distance of 0.1 m from the target lane center line, see Figure 6. At 78 km/h the DMC completes the lane change at 39 s and the NMPC at 32 s, see Figure 8. At the velocity of 44 km/h, the maximum absolute value of the steering wheel amplitude during the manoeuvre is lower for the DMC than for the NMPC, at approximately 16 and 22 °, respectively, see Figure 7. However, the DMC's initial steering rate is higher than that of the NMPC. The DMCs lateral control was parametrized for constant speed at 80km/h, see Section IV-A2. For the DMC, the maximum absolute lateral accelerations of the 1st and 11th LVC axles as well as the rearward amplification are slightly lower than for the NMPC. At the velocity of 78 km/h the maximum absolute value of the steering wheel amplitude during the manoeuvre is higher for the DMC than for the NMPC, at approximately 14 and 9 °, respectively, see Figure 9. Again, the initial DMC's steering rate is higher than that of the NMPC. For the DMC, the maximum absolute lateral accelerations of the 1st and 11th LVC axles, as well as the rearward amplification are slightly higher than for the NMPC.

B. Scenario II: Lane change combined with braking

In this section the performance of the DMC and the NMPC are compared for lane changes combined with braking at the
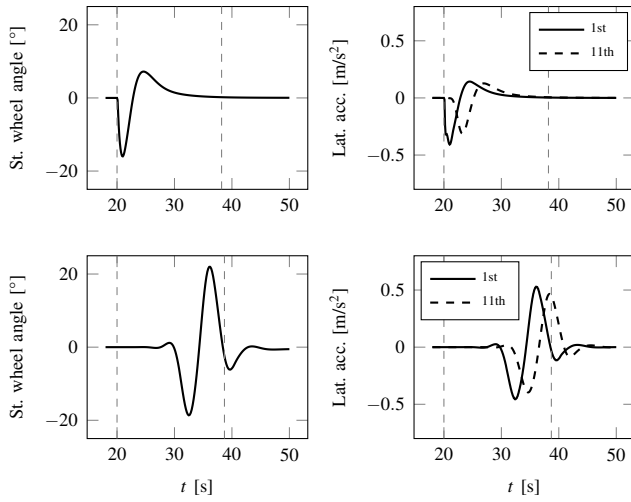
Fig. 7: Characteristics of a lane change at the constant velocity of 44 km/h: steering wheel angle DMC (top left), lateral acceleration DMC (top right), steering wheel angle NMPC (bottom left), and lateral acceleration NMPC (bottom right). The dashed vertical lines indicate lane change initiation and completion.
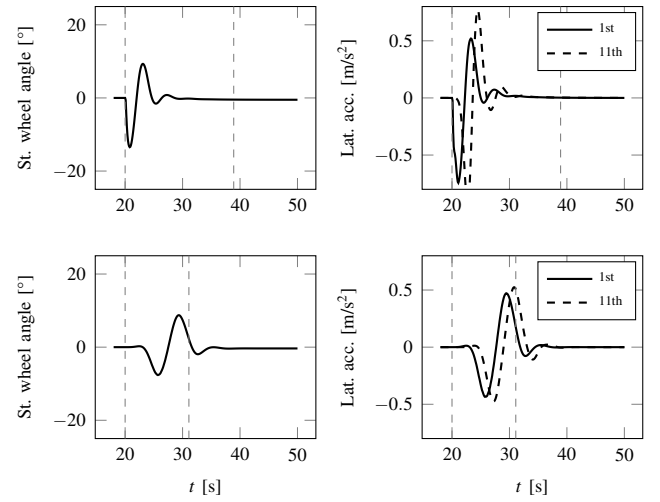
Fig. 9: Characteristics of a lane change at the constant velocity of 78 km/h: steering wheel angle DMC (top left), lateral acceleration DMC (top right), steering wheel angle NMPC (bottom left), and lateral acceleration NMPC (bottom right). The dashed vertical lines indicate lane change initiation and completion.
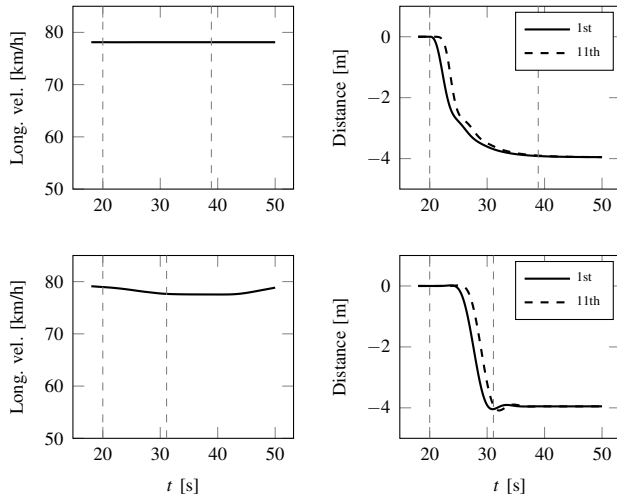
Fig. 8: Characteristics of a lane change at the constant velocity of 78 km/h: vehicle speed DMC (top left), lane center distance offset DMC (top right), vehicle speed NMPC (bottom left), and lane center distance offset NMPC (bottom right). The dashed vertical lines indicate lane change initiation and completion.
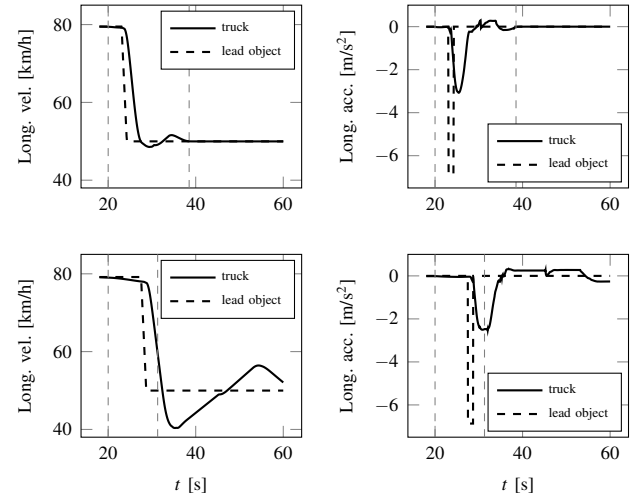
Fig. 10: Characteristics of a lane change combined with braking where the initial and final velocities are 80 km/h and 50 km/h, respectively: longitudinal velocity DMC (top left), longitudinal acceleration DMC (top right), longitudinal velocity NMPC (bottom left), and longitudinal acceleration NMPC (bottom right). The initial headway is 2 s.

initial and final velocities of 80 and 50 km/h, respectively. The initial headway to the lead vehicle is 2 s and the lead vehicle deceleration is varied in the range of 0.1-0.7 g. The important characteristics of a lane change combined with lead vehicle braking at 0.7g are illustrated in Figures 10-11.

At time 20 s, the LVC velocity is 80 km/h and a lane change to right is requested. At time 23 s for the DMC and 27.5 s for the NMPC, the LVC front axle enters the target lane and the leading vehicle brakes from 80 to 50 km/h using a deceleration of 0.7 g. During the LVC braking, the maximum deceleration reaches 3.1 and 2.5 m/s^2 for the DMC and NMPC, respectively. The deceleration in the NMPC is limited by the constraint on maximum deceleration, see Table I. The minimum velocities

of the LVC are 49 and 40 km/h, see Figure 11. For the DMC, the maximum absolute lateral accelerations of the 1st and 11th LVC axles, as well as the rearward amplification, are higher in comparison to the NMPC. The reason for this is most likely that the initial steering rate of the DMC lateral control is closer to the important resonance frequency of the LVC.

In Figure 12, the longitudinal and lateral accelerations of the LVC front axle are illustrated in acceleration diagrams. At Point (1), the lane change is requested and at Point (2) the LVC front axle enters the target lane and the leading vehicle starts to decelerate. At Point (3) the lane change is completed and at Point (4) the LVC has adapted to the velocity of the leading
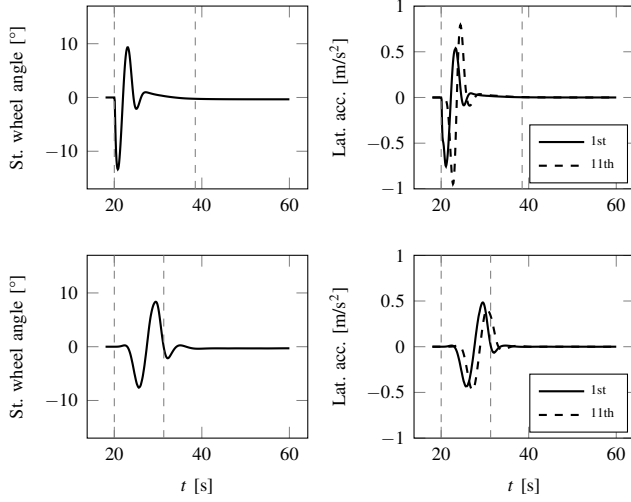
Fig. 11: Characteristics of a lane change combined with braking where the initial and final velocities are 80 km/h and 50 km/h, respectively: steering wheel angle DMC (top left), lateral acceleration DMC (top right), steering wheel angle NMPC (bottom left), and lateral acceleration NMPC (bottom right). The initial headway is 2 s.
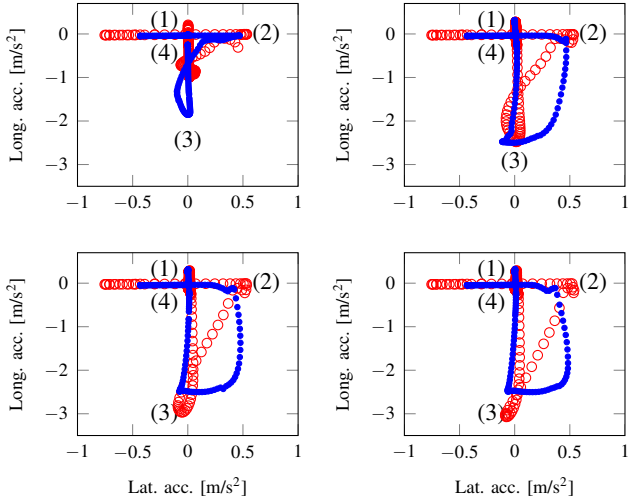
Fig. 12: Acceleration diagrams of the longitudinal and lateral accelerations of the LVC front axle during the lane change manoeuvres: leading vehicle deceleration 0.1 g (top left), leading vehicle deceleration 0.3 g (top right), leading vehicle deceleration 0.5 g (bottom left), and leading vehicle deceleration 0.7 g (bottom right). The DMC is represented by red circles and NMPC by blue filled circles.

vehicle. It is noted that the maximum lateral accelerations of the DMC are higher than those of the NMPC in all cases. The maximum longitudinal decelerations of the DMC are also higher than the NMPC in all cases except when the leading vehicle deceleration is 0.1 g. The shape of the graphs for the DMC and the NMPC are diverse, indicating a different steering and braking behaviour during the lane change manoeuvre. The NMPC does more simultaneous braking and steering while the DMC steers first and then brakes.

VI. CONCLUSIONS AND DISCUSSION

This paper compares the vehicle dynamics performance of two specific approaches for automated lane change manoeuvres of an A-double LVC in emulated highway traffic. The results show that both approaches are able to perform feasible lane change manoeuvres at the constant speeds of 44 and 78 km/h. In addition, lane changes were successfully conducted when combined with deceleration due to leading vehicle braking from 80 to 50 km/h with a varying deceleration range of 0.1-0.7 g. In all simulations, the DMC lateral control shows excessive levels of the initial steering wheel rate. This behaviour is most likely related to that the driver model, originally formulated by Salvucci and Gray [19], was developed for corrective manoeuvres. A corrective manoeuvre encompasses some urgency to return to the lane center which is not the case in a normal lane change. Also, the steering behaviour of the DMC at 44 km/h does not exhibit the characteristic sine-wave pattern that is commonly seen in a lane change manoeuvre [24]. The reason for this is probably due to the fact that the parameters of the driver model have been obtained for lane changes at 80 km/h. One viable option for improving the steering performance of the DMC for a wider range of scenarios, is to use on-line optimization of driver model parameters e.g by using particle swarm optimization solver techniques. The NMPC controller initiates the lane changes 1 to 8 s after the lane changes were requested. The delay was introduced in order to allow the RTI scheme to adapt its solution in a controlled manner and to avoid highly suboptimal solutions. Also, the longitudinal speed adjustment of NMPC is more varying than that of the DMC. Both the deflective steering behaviour of the DMC as well as the lane change initiation delay and the varying speed adjustment of the NMPC can have an impact on the satisficing behaviour for the human occupant. In general, the NMPC shows shorter lane change duration times and lower values of the used absolute magnitude of the longitudinal and lateral accelerations.

APPENDIX

In the prediction of traffic situations the given differential equations are used to describe the LVC motion in the lane

$$\dot{z}_1 = 47.0 \cdot \delta - z_{10} \cdot z_3 + 1.9 \cdot z_4 + 0.9 \cdot z_6 - 0.002 \cdot z_8$$
$$+ (-70.7 \cdot z_1 + 9.7 \cdot z_3 + 21.7 \cdot z_5 + 4.5 \cdot z_7 - 0.02 \cdot z_9)/z_{10}$$
$$\dot{z}_2 = z_3 - \kappa_{R,1} \cdot (z_{10} \cdot \cos(z_2) - (z_1 + z_3 \cdot 1.5) \cdot \sin(z_2))$$
$$\dot{z}_3 = 25.0 \cdot \delta - 1.9 \cdot z_4 - 0.8 \cdot z_6 + 0.002 \cdot z_8 + (27.6 \cdot z_1$$
$$- 174.2 \cdot z_3 - 20.8 \cdot z_5 - 4.3 \cdot z_7 + 0.02 \cdot z_9)/z_{10}$$
$$\dot{z}_4 = z_5$$
$$\dot{z}_5 = -25.5 \cdot \delta - 4.0 \cdot z_4 + 2.5 \cdot z_6 - 0.007 \cdot z_8 + (-36.5 \cdot z_1$$
$$+ 165.4 \cdot z_3 - 10.9 \cdot z_5 + 13.0 \cdot z_7 - 0.05 \cdot z_9)/z_{10}$$
$$\dot{z}_6 = z_7$$
$$\dot{z}_7 = 0.6 \cdot \delta + 2.3 \cdot z_4 - 22.9 \cdot z_6 - 0.9 \cdot z_8 + (19.9 \cdot z_1$$
$$- 216.8 \cdot z_3 - 169.7 \cdot z_5 - 125.8 \cdot z_7 - 7.2 \cdot z_9)/z_{10}$$
$$\dot{z}_8 = z_{10}$$
$$\dot{z}_9 = -0.19 \cdot \delta + 5.1 \cdot z_4 + 22.7 \cdot z_6 - 7.1 \cdot z_8 + (-12.5 \cdot z_1$$
$$- + 195.8 \cdot z_3 + 168.6 \cdot z_5 + 68.2 \cdot z_7 - 54.7 \cdot z_9)/z_{10}$$
$$\dot{z}_{10} = a_{x,1}$$
$$\dot{z}_{11} = (a_{x,1,\text{des}} - a_{x,1})/\tau$$
$$\dot{z}_{12} = 1/(1 - \kappa_{R,1} \cdot z_{13}) \cdot (z_{10} \cdot \cos(z_2) - (z_1 + z_3 \cdot 1.5) \cdot \sin(z_2))$$
$$\dot{z}_{13} = z_{10} \cdot \sin(z_2) + (z_1 + z_3 \cdot 1.5) \cdot \cos(z_2)$$

$$\dot{z}_{14} = 1/\left(1 - \kappa_{R,4} \cdot z_{15}\right) \cdot \left(\left(-24.6 \cdot z_3 - 22.7 \cdot z_5 - 12.3 \cdot z_7 - 7.7 \cdot z_9\right.\right.$$
$$-z_4 \cdot z_{10} - z_6 \cdot z_{10} - z_8 \cdot z_{10} + z_1\right) \cdot -\sin\left(z_2 + z_4 + z_6 + z_8\right.$$
$$\left.-\theta_{R,4} + \theta_{R,1}\right) + z_{10} \cdot \cos\left(z_2 + z_4 + z_6 + z_8 - \theta_{R,4} + \theta_{R,1}\right)\right)$$
$$\dot{z}_{15} = \left(\left(-24.6 \cdot z_3 - 22.7 \cdot z_5 - 12.3 \cdot z_7 - 7.7 \cdot z_9 - z_4 \cdot z_{10} - z_6 \cdot z_{10}\right.\right.$$
$$-z_8 \cdot z_{10} + z_1\right) \cdot \cos\left(z_2 + z_4 + z_6 + z_8 \theta_{R,4} + \theta_{R,1}\right) + z_{10} \cdot \sin\left(z_2 + z_4\right.$$
$$\left.\left.+z_6 + z_8 - \theta_{R,4} + \theta_{R,1}\right)\right)$$
$$\dot{z}_{16} = \dot{\delta}$$
$$z = \left[\dot{y}_1, \phi, \dot{\phi}, \theta_1, \dot{\theta}_1, \theta_2, \dot{\theta}_2, \theta_3, \dot{\theta}_3, v_{x,1}, a_{x,1}, s_1, e_1, s_{11}, e_{11}, \dot{\delta}\right]$$
$$u = [a_{x,1,\text{des}}, \delta]$$

The states $\dot{y}_1$, ϕ and $\dot{\phi}$ are the lateral velocity, yaw angle and yaw rate of the first vehicle axle. $\theta_1, \theta_2, \theta_3, \dot{\theta}_1, \dot{\theta}_2$ and $\dot{\theta}_3$ are the articulation angles and the rate of the articulation angles of the towed units. $v_{x,1}$ and $a_{x,1}$ are the longitudinal velocity and acceleration of the first vehicle axle. s_1, s_{11}, e_1 and e_{11} are the distances and the perpendicular distances of the first and the last vehicle axles projected on the lane geometry. The variables $\kappa_{R,1}, \kappa_{R,4}, \theta_{R,1}, \theta_{R,4}$ are the road curvature and heading angles of the first and last vehicle axles. The parameter τ is a constant for the longitudinal dynamics. The inputs are the longitudinal acceleration of the first vehicle axle $a_{x,1,\text{des}}$ and the road wheel steering angle δ. All units are SI.

The motion of the surrounding vehicles are given as

$$\frac{d}{dt}\begin{bmatrix} s_{o,n} \\ \dot{s}_{o,n} \end{bmatrix} = \begin{bmatrix} 0 & 1 \\ 0 & 0 \end{bmatrix} \cdot \begin{bmatrix} s_{o,n} \\ \dot{s}_{o,n} \end{bmatrix} + \begin{bmatrix} 0 \\ 1 \end{bmatrix} \cdot \ddot{s}_{o,n}$$

$n = 1, ..., 6$ are the number of surrounding vehicles

where $s_{o,n}, \dot{s}_{o,n}$ and $\ddot{s}_{o,n}$ are the position, velocity and acceleration tangential to the defined road geometry.

ACKNOWLEDGMENT

REFERENCES

[1] M. S. Kati, "Definitions of performance based characteristics for long heavy vehicle combinations," Chalmers University of Technology, Tech. Rep., 2013.

[2] H. Summala, "Towards understanding motivational and emotional factors in driver behaviour: Comfort through satisficing," in *Modelling Driver Behaviour in Automotive Environments*, P. Cacciabue, Ed. Springer London, 2007, pp. 189–207.

[3] P. Hart, N. Nilsson, and B. Raphael, "A formal basis for the heuristic determination of minimum cost paths," *Systems Science and Cybernetics, IEEE Transactions on*, vol. 4, no. 2, pp. 100–107, 1968.

[4] R. M. Rosenberg, *Analytical Dynamics of Discrete Systems*. Springer US, 1977.

[5] J. Frasch, A. Gray, M. Zanon, H. Ferreau, S. Sager, F. Borrelli, and M. Diehl, "An auto-generated nonlinear mpc algorithm for real-time obstacle avoidance of ground vehicles," in *Control Conference (ECC), 2013 European*, 2013, pp. 4136–4141.

[6] S. M. LaValle and J. J. Kuffner, "Randomized kinodynamic planning," *The International Journal of Robotics Research*, vol. 20, no. 5, pp. 378–400, 2001.

[7] J. Sandin, P. Nilsson, B. Augusto, and L. Laine, "A lane-change gap acceptance scenario developed for heavy vehicle active safety assessment: A driving simulator study," 2015, submitted to FAST-zero 2015 Symposium, Gothenburg.

[8] N. van Duijkeren, T. Keviczky, P. Nilsson, and L. Laine, "Real-time nmpc for semi-automated highway driving of long heavy vehicle combinations," 2015, submitted to 5th IFAC Conference on Nonlinear Model Predictive Control Seville, September 17-20, 2015, Spain.

[9] P. Nilsson, L. Laine, and B. Jacobson, "Performance characteristics for automated driving of long heavy vehicle combinations evaluated in motion simulator," in *Intelligent Vehicles Symposium Proceedings, 2014 IEEE*. IEEE, 2014, pp. 362–369.

[10] P. Nilsson and K. Tagesson, "Single-track models of an A-double heavy vehicle combination," Chalmers University of Technology, Tech. Rep. 8, 2013.

[11] H. B. Pacejka, *Tire and vehicle dynamics*. Butterworth-Heinemann, 2006.

[12] J. S. Albus, "4d/rcs: a reference model architecture for intelligent unmanned ground vehicles," in *Proc. SPIE*, vol. 4715, 2002, pp. 303–310.

[13] J. Schröder, D. Holzner, C. Berger, C.-J. Hoel, L. Laine, and A. Magnusson, "Design and evaluation of a customizable multi-domain reference architecture on top of product lines of self-driving heavy vehicles - an industrial case study," in *37th International Conference on Software Engineering (ICSE 2015)*, 2015.

[14] L. Laine, "Reconfigurable motion control systems for over-actuated road vehicles," Ph.D. dissertation, Chalmers University of Technology, 2007.

[15] K. Tagesson, P. Sundstrom, L. Laine, and N. Dela, "Real-time performance of control allocation for actuator coordination in heavy vehicles," in *Intelligent Vehicles Symposium, 2009 IEEE*, 2009, pp. 685–690.

[16] K. Uhlen, P. Nyman, J. Eklöv, L. Laine, M. Sadeghi Kati, and J. Fredriksson, "Coordination of actuators for an a-double heavy vehicle combination using control allocation," in *Intelligent Transportation Systems (ITSC), 2014 IEEE*, 2014, pp. 641–648.

[17] P. Nilsson, L. Laine, B. Jacobson, and N. van Duijkeren, "Driver model based automated driving of long vehicle combinations in emulated highway traffic," 2015, submitted to IEEE 18th International Conference on Intelligent Transportation Systems (ITSC), September 15-18, 2015. Las Palmas, Spain.

[18] D. Lee, "A theory of visual control of braking based on information about time to collision," *Perception*, vol. 5, no. 4, pp. 437–459, 1976.

[19] D. D. Salvucci and R. Gray, "A two-point visual control model of steering," *Perception*, vol. 33, pp. 1233–1248, 2004.

[20] J. H. Holland, *Adaptation in natural and artificial systems: An introductory analysis with applications to biology, control, and artificial intelligence*. U Michigan Press, 1975.

[21] P. Nilsson, L. Laine, O. Benderius, and B. Jacobson, "A driver model using optic information for longitudinal and lateral control of a long vehicle combination," in *Intelligent Transportation Systems (ITSC), 2014 IEEE 17th International Conference on*, 2014, pp. 1456–1461.

[22] M. Diehl, H. G. Bock, and J. P. Schlöder, "A real-time iteration scheme for nonlinear optimization in optimal feedback control," *SIAM Journal on Control and Optimization*, vol. 43, no. 5, pp. 1714–1736, 2005.

[23] B. Houska, H. J. Ferreau, and M. Diehl, "An auto-generated real-time iteration algorithm for nonlinear mpc in the microsecond range," *Automatica*, vol. 47, no. 10, pp. 2279–2285, 2011.

[24] D. D. Salvucci and A. Liu, "The time course of a lane change: Driver control and eye-movement behavior," *Transportation Research Part F: Traffic Psychology and Behaviour*, vol. 5, no. 2, pp. 123–132, 2002.